Chapter 03: Materials and Experimental Details

3.1 Introduction

This chapter of the thesis describes various experimental techniques utilized to carry out the investigations. A brief outline of various processing routes used for the synthesis of MGs/MGs-composites. Three different processing routes synthesize all four alloys. They refer to, (i) arc-melting followed by Cu-mould casting, (ii) Melt spinning, and (iii) high-energy ball milling techniques. Consolidation of ball-milled powders after 100h of milling has been done by using the spark plasma sintering technique (SPS). The bulk density of the materials was measured by the simple Archimedes principle. The microstructures of samples under various conditions were investigated by optical microscopy (OM). The structural characterization techniques, including X-ray diffraction and transmission electron microscope (TEM) (imaging and diffraction mode), were used. The scanning electron microscopy (SEM) technique using secondary electrons (SE) was used for surface morphology and chemical analysis of microstructural features with the help of Energy Dispersive X-ray Spectroscopy (EDAX). The thermal characterization of materials was done by the differential scanning calorimetry (DSC) instrument. The micro-indentation technique for the determination of the hardness of alloys, MGs, and MGs-composites will be described in subsequent sections.

3.2 Materials Systems

The material systems that have been chosen in the present study can be categorized into two parts: (i) Metals (Fe, Mo, Cr, Y, W, and Co), and (ii) Metalloids (B, C, and Si). Four Fe-based alloys, whose composition was selected from the literature on the basis of the Venn diagram model (e/a, V_R, and R_R criteria) for MGs formation. This has been dealt with in chapter 02. The master alloy utilized for making them was grey cast iron (C.I.). The required amounts of elements in bulk form were added to this cast iron to get nominal compositions given in Table 3.1. The alloys are designated as A, B, C, and D. The common elements added to make them are Mo (Alfa Aesar, 99.95%) in the form of rod (3mm diameter), Cr (Alfa Aesar, 99.9%) in the form of lumps in irregular shape of 5mm in size, B (Sigma Aldrich,99.7%) in the form of crystalline irregular pieces of 10mm in size. In addition to these we have added Y (Alfa Aesar) in the form of irregular pieces of 20mm size, W (Alfa-Aesar, 99.9%) in the form of rod (5mm diameter), and Co (Alfa-Aesar,99.8%) in the form of cuboid ($5x5x5mm^3$) are added in alloys C, and D respectively. The

physical properties of all the elements used for synthesis in the present investigation are mentioned in Table 3.2.

Table 3. 1: The master alloy composition and nominal compositions with various parameters

Master Alloy of C. I	**Elements**	**C**	**Si**	**P**	**S**	**Fe**
	Atom%	15.34	4.05	0.187	0.167	Balance
Alloy designation	Nominal composition (at %)			**e/a**	**V_R**	**R_R**
A	$Fe_{56.24}Cr_4Mo_{14}C_{15}Si_{3.8}B_6$			2.17	0.66	1.61
B	$Fe_{43.47}Cr_{15}Mo_{14}C_{15.12}Si_{3.78}B_6Y_2$			1.67	0.47	2.33
C	$Fe_{40.2}Cr_{20}Mo_{10}W_2C_{15}Si_{4.2}B_6Y_2$			1.33	0.11	2.33
D	$Fe_{40.2}Cr_{15}Mo_{14}Co_3C_{15}Si4._2B_6Y_2$			1.74	0.12	2.33

Table 3. 2: Physical properties of elements used for synthesis of alloys, composites, and amorphous alloys.

Elements	**Fe**	**Cr**	**Mo**	**W**	**Co**	**Y**	**C**	**B**	**Si**
Density (g/cc)	7.86	7.19	10.28	19.25	8.92	4.47	2.20	2.46	2.33
Melting point (^OC)	1538	1907	2623	3370	1495	1522	3500	2300	1414
Crystal structure	BCC	BCC	BCC	BCC	HCP	HCP	hexagonal	rhombohedral	DC

3.3 Materials Synthesis Techniques

Three processing routes are employed, which are a part of the studies of this thesis. These processing routes are as follows:

(i) Cu-mould casting

(ii) Melt-spinning technique

(iii) High-energy ball milling

Further, 100h of ball-milled powders are consolidated by the spark plasma sintering (SPS) technique.

3.3.1 Cu-mould casting Technique

To make alloys, Vacuum arc melting was used for melting followed by the Cu-mould casting technique. These alloys will be termed as cast alloys. One of the valiant of this technique has been used for the synthesis of Bulk Metallic Glasses (BMGs)[4], [15]. It imparts a low critical cooling rate required for the formation of a glassy phase. This technique requires arc melt of the alloy on the Cu-hearth. Once the metals are melted, the Cu-hearth acts like a heat sink, and heat is extracted from molten alloys. The argon gas was used for the desired melting purpose. An optical image of the arc melting furnace unit is shown in Fig.3.1(a)-(b). Fig.3.1(a) represents the inside chamber of the arc melting furnace that contains Cu-hearth where samples are to be kept for melting and a tungsten electrode was used for generating the arc. Fig.3.1(b) shows the complete set-up unit of the arc-melting furnace. This arc melting furnace set-up has a suction casting attachment too, but we have used only a simple Cu-hearth arc melting process (make: M/S Vacuum Technologies, Bangalore).

This technique is also analogous to the conventional casting of alloys in a metal mold [149], [150]. In the microstructure of arc-cast alloys, one can visualize three different zones of solidification like conventional casting (chill zone, columnar zone, and equiaxed zone). In the chill zone (direct contact with the mold wall) the alloy experiences very high under-cooling, hence extremely fine grains are formed. A columnar structure forms due to the inverse temperature gradient in liquid ahead of the solid-liquid interface. In the case of the central equiaxed zone a glassy phase forms in the inner region where the heat flux is reinforced from the Cu-hearth. Although the cooling rate is reduced in this region, this low cooling rate is sufficient for some alloys to become glassy. The optical micrograph of arc-melt cast samples represents the presence of chill zone, columnar zone clearly at the edges of casted alloys and the glassy phase at the centre of casting[151].

The serious drawback of this technique is that it is very difficult to entirely avoid the formation of a small amount of crystalline phase that is formed on the surface. This drawback comes due to heterogeneous nucleation of incomplete melting of the alloy at the bottom side that is in contact with the Cu-hearth.

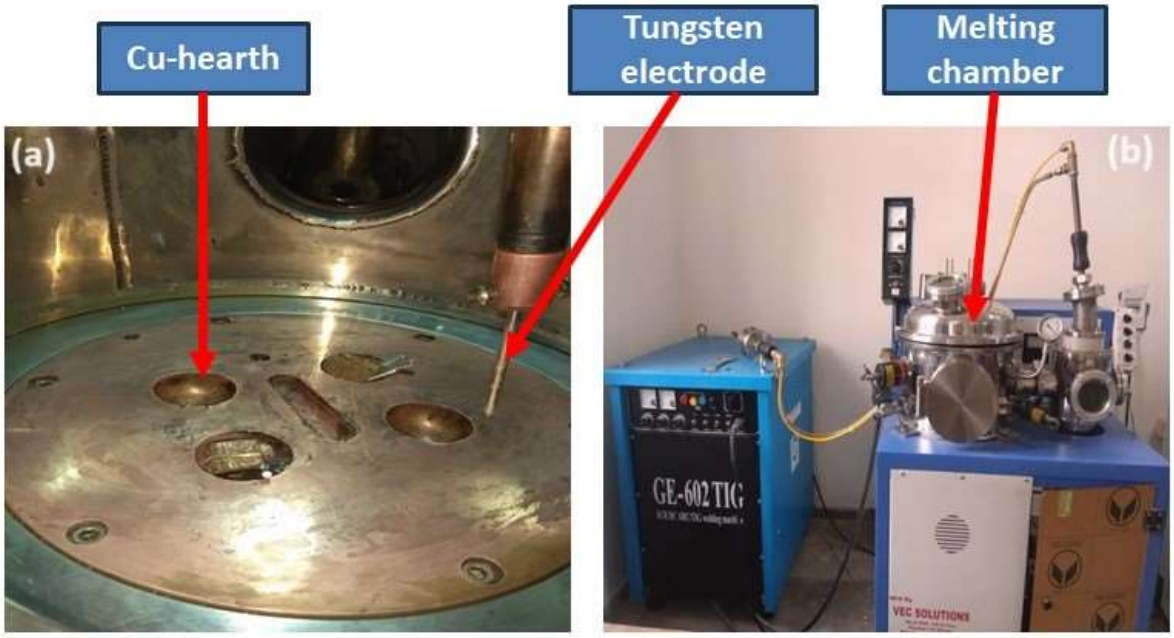

Fig. 3. 1: The Optical picture of Arc melting furnace unit with Cu-hearth

In the present investigation for the synthesis of alloys or nanocrystalline alloys, a vacuum arc melting followed by Cu-mould casting has been used. The required stoichiometric quantities of raw materials were melted in Cu-hearth. Once the complete melting of charge is done, then melts are allowed to solidify in the Cu-hearth. A tungsten electrode was used for generating the arc under the argon atmosphere. Ti-gutters are used to avoid oxidation. Alloys are formed in the form of buttons having 30mm diameter and 10mm thickness.

3.3.2 Melt-spinning Technique

The melt spinning technique has been most famous and widely used to produce long and continuous rapidly solidified ribbons, wires, and filaments. The melt-spinning technique involves the extrusion of molten metal to produce fine ribbons or filaments in such a way that can be used directly. In the melt-spinning technique, a small quantity of alloy is melted inside a crucible and then ejected under pressure through a fine nozzle or orifice onto a fast-rotating Cu wheel. All the melt-spinning parameters can be carefully controlled to get the desired size, shape, and thickness of melt-spun ribbons. A schematic picture of the melt-spinning process is shown in Fig.3.2. The primary objective of the rapid solidification process (RSP) is avoiding limitations associated with conventional materials solidification processing. A very high cooling rate such as 10^5-10^6 K/s is

required to avoid the propagation of nucleation of high temperature equilibrium phases. In order to get a very high cooling rate through a specimen, its dimensions should be very small at least in one direction. The alloy product comes out in the form of ribbons.

The crucible materials are chosen based on their chemical compatibility with the liquid melt such as their low thermal conductivity, temperature handling capability, resistance to thermal shock, and low porosity. Generally, the three most common materials quartz, graphite, and dense alumina are used in making the crucibles. The wheels for melt-spinning have been made from a variety of materials such as including copper, stainless steel, molybdenum, and chromium. Although Copper is the most popular material to make melt-spinning rotating wheels. The melt-spinning process can be carried out in air, vacuum, or inert atmosphere.

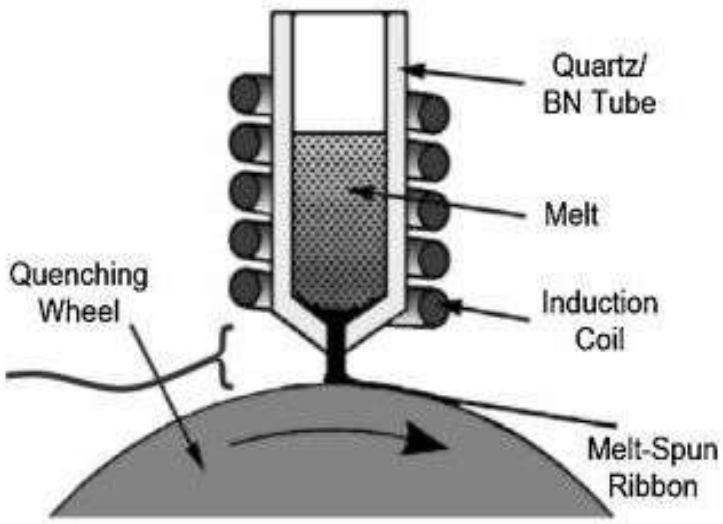

Fig. 3. 2: A schematic illustration of the melt-spinning technique

The RSP technique can be used in various types of applications other than the glassy phase such as synthesis of quasi-crystalline materials, high-temperature materials, high-strength structural materials, corrosion resistance, storage materials, and electrical or magnetic materials.

In the present investigation of the synthesis of ribbons in the form of metallic glasses and metallic-glass composites, the melt-spinning technique has been used. I have used two different melt-spinners with different rotating wheel speeds and crucibles for the synthesis of ribbons. The complete information regarding the melt-spinning parameter is mentioned in Chapter 5. The required quantity of the as-cast alloys was sliced and placed inside the crucibles, which were properly fixed within the induction coil. The nozzle of the crucible was aligned such that the melt flowed onto to rotating Cu wheel when ejected. The Cu wheel was water-cooled and was finely

polished with the abrasive paper before the melt-spinning operation started. There are following factors that affect the cooling rate and thickness of the ribbons and need to be optimized for the synthesis of a good quality ribbon. These parameters are as follows:

(i) Rotating speed of the wheel (the average thickness decreases as wheel speed increases).
(ii) The gas (Argon gas) pressure that is used to push the molten alloys through the nozzle.
(iii) The striking angle of the melt jet with the wheel.
(iv) Thermal conductivity, temperature, and the surface smoothness of the wheel (an increment of wheel temperature will increase the average thickness of ribbons and also morphology get change).
(v) Diameter of orifice of the nozzle.

3.3.3 High-Energy Ball milling Technique

Mechanical milling (MM) or mechanical alloying (MA) are other popular techniques that have been extensively used for the synthesis of several alloys and composites with equilibrium or metastable structures at room temperature[152]. The most interesting feature of MM/MA is the ability to synthesize amorphous and nanocrystalline materials. In this technique, material involves continuous ball milling of powders. The ball milling process has the following steps which are shown in Fig. 3.3 (a)-(b). The severe plastic deformation, repeated flattening, cold welding, and fracturing of powder particles during MM or MA technique leads to the significant refinement of microstructure as shown in Fig.3.3 (a). The microstructure refinement depends on the mechanical properties of initial powders or alloys, the types of mills used, the ball-to-powder weight ratio, and the temperature at which milling is carried out. The final powder of the ball milled has metastable structures. The best advantage of MM/MA is it can provide microstructures that are impossible or very difficult to obtain with other techniques. It can overcome fabrication difficulties in achieving high solid solubility, mixing of elements with high vapor pressure, or large differences in melting points.

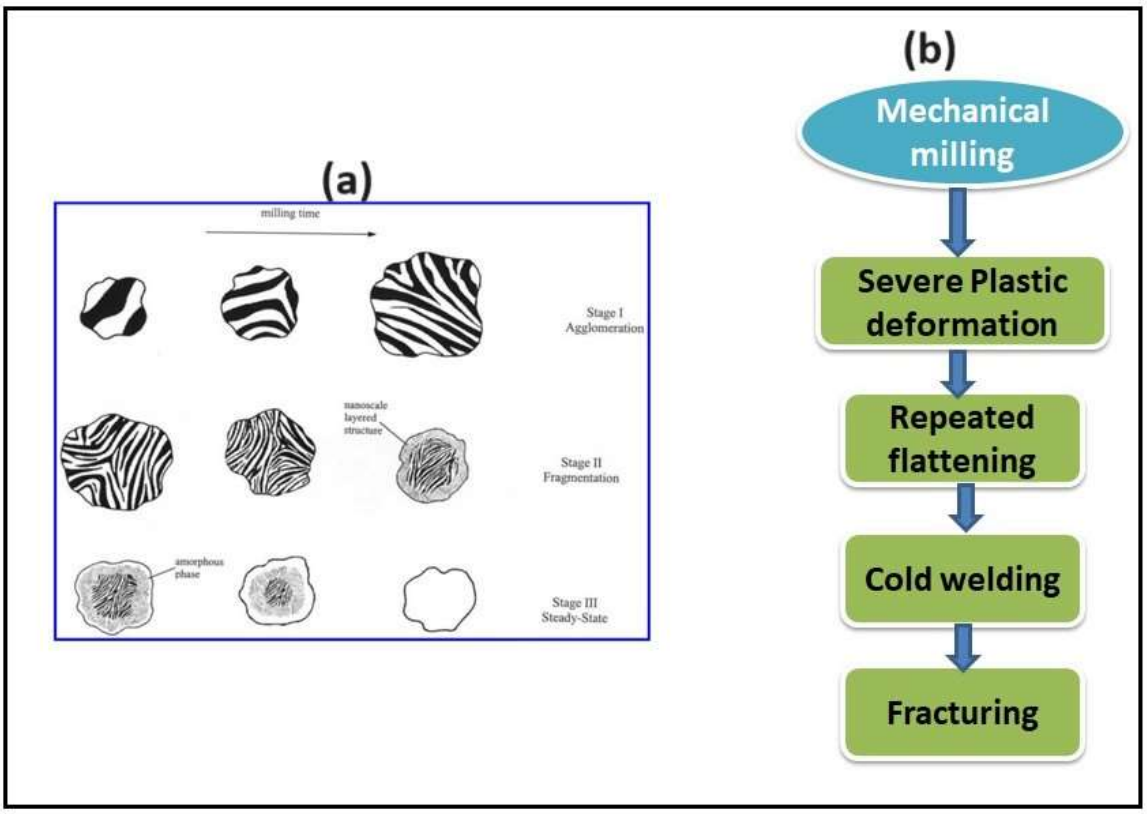

Fig. 3. 3: (a) Schematic representation of the evolution of powder morphology and microstructures developed during MM/MA [152], (b) A Flow diagram represents various steps in the MM process**.**

In the present investigation, the synthesis of nanocomposite powders was obtained by using a high-energy planetary ball mill (Retsch, PM400/2) at a speed of 200 rpm. The required quantity of as-cast alloys was taken and crushed into small granules in order of ~1mm. The ratio of ball to powder (BPR) was taken at 10:1. The milling was carried out in tungsten carbide (WC) vials with tungsten carbide balls. To avoid oxidation and heating effect toluene was used as a processing control reagent (PCA). The milling operation was stopped intermittently for 30 min after every 1h of milling to avoid overheating. The alloys were milled for up to 120h duration. The process parameters for the milling operation are summarized in Table 3.3.

Table 3. 3: Detail information regarding ball-milling nanocomposite powders

Sample designation	**Milling duration**	**Sample Withdrawal duration**	**Vials and balls**	**Milling medium**	**Process control reagent**
BMP-A	120h	30h,40h, 70h,100h, 120h	WC	Wet	Toluene
BMP-B	120h	10h,50h, 70h,100h, 120h	WC	Wet	Toluene
BMP-C	120h	20h,40h, 60h,80h, 100h, 120h	WC	Wet	Toluene
BMP-D	120h	20h,40h, 60h,80h, 100h,120h	WC	Wet	Toluene

3.3.4 Spark plasma sintering (SPS) Technique

Sintering is the process of making objects through the consolidation of powders by applying heat to the material in a furnace below its melting temperature for very few durations. The bonding between the particles takes place by diffusion of atoms. SPS is an advanced technique that takes only a few minutes to complete a sintering process. A high sintering rate is possible in SPS since high heating rates can be easily attained due to the internal heating of samples. In the SPS process the powder is fed directly into the graphite dies and the die is enclosed with suitable punches. The entire assembly is directly put inside the SPS chamber. Now, the chamber is closed and argon gas was used to create a vacuum inside the chamber. The program is set into the control unit and a sintering operation is carried out. All types of materials can be easily sintered and densified by this technique. The best advantage of SPS is due to the high heating rate and less holding time can

restrict the unwanted sintering reactions in highly reactive systems, hence formation of undesirable phases can be avoided.

In the present work for densification of nanocomposite powders are designated as BMP-A, BMP-B, BMP-C, and BMP-D. I have taken 10g of each composition of 100h ball-milled powders for consolidation. The consolidation of 100h nanocomposite powders was carried out using spark plasma sintering equipment (SPS 1000: Suga Co. Ltd., Japan). The milled powder samples are kept in a cylindrical graphite die. The die line is covered with a graphite sheet for easy removal of the sintering compact. The die containing the powder sample was kept inside the SPS chamber and set the time-temperature program. It takes some time for the creation of a vacuum (10^{-3} Torr) atmosphere inside the chamber. Argon gas was purged inside the SPS chamber at a gas flow rate of 5 L/min. A high DC pulse is passed between graphite electrodes and axial pressure is simultaneously applied from the commencement of the sintering cycle. The sample is heated by the joules heating and the sparking among the particles of sintered materials leads to the faster heat and mass transfer. After the completion of sintering, the power is turned off and the sample is allowed to cool up to room temperature. The processing parameters for compaction of 100h ball-milled nanocomposite powders are mentioned in Table 3.4.

Table 3. 4: Processing parameters for compaction of ball-milled powder composite by SPS technique

Sample designation	Temperature (ºC)	Pressure (MPa)	Heating rate (ºC/min)	Holding time (in min.)	Diameter Pellets (mm)	Thickness of pellets (mm)
SPSed-A	800	50	100	15	10	5
SPSed-B	800	50	100	15	10	10
SPSed-C	800	50	100	15	10	5
SPSed-D	800	50	100	15	10	5

3.3.5 Heat Treatment: Annealing Experiment

In the study of the controlled crystallization behavior of metallic glasses, a resistance heating furnace has been used. The temperature variation of this furnace is ± 5ºC. The ribbon samples were heated up to 635ºC (908K)-645ºC (918K) temperature and then kept for 1h for isothermal

treatment and was switched off the furnace after 1h heating at constant temperature and then allow it to cool at room temperature. The samples were left inside the chamber for one day. In the case of vacuum, the annealing samples were sealed in a quartz tube with a tube diameter of ~20mm diameter and filled with argon atmosphere.

3.4 Techniques Used for Characterization

3.4.1 Density Measurement

The Archimedes principle was used for the measurement of the density of as-cast and sintered samples. An electronic weighing balance (Model no.-CAH-503, CONTECH Instrument Ltd., Mumbai, India) attached with a density measurement module was used for this purpose. Initially sample was weighted in air and then liquid (distilled water) medium. The density of the samples was measured by the following expression.

3.4.2 Optical Microscopy (OM): Microstructure Analysis

An optical microscope (Leica model LV 500) was used for the microstructure characterization of as-cast alloys, melt-spun ribbons, and sintered alloys. Samples are polished by using standard metallography techniques. The first samples were cold-mounted by using Bakelite powder. Samples were first flattened by mechanical grinding, and cloth polishing and then polished with 200, 600, 1000, and 1200 grit size silicon carbide paper. Finally, fine polishing was done on a Trident and Chemo Met cloth (trademark of Buehler) with 0.5µm diamond suspension and colloidal silica (0.02µm). After polishing these samples were etched with 5% nital (vol.%) solution for revealing their microstructures.

3.4.3 X-ray Diffraction (XRD) Technique: Structural and Phase Analysis

The investigation of structure and phases evolve in as-cast, ball-milled, and annealed ribbon samples was carried out X-ray diffraction (MiniFlex600, RIGAKU) instrument using Cu-K_α (λ=1.541A^o) radiation source. The operating voltage and current were kept at 40kV and 15mA respectively. The diffractometer was calibrated by using single crystal silicon powder as a standard for obtaining accurate 2θ value for the calculation of lattice parameters. All the samples are cut in the required shape and put on the sample holder. All the samples were scanned from 2θ=20 to 100^o angle with a step size of 0.02^o with 5^o/min scan speed.

In the present investigation, the average crystallite size (t) and micro-strain (ε) were calculated by using Williamson-Hall(W-H) method[153] by applying the expression as discussed below.

$$\beta^{*}Cos\theta = 0.9^{*}\lambda/t + 4\varepsilon^{*}sin\theta$$

Where t= Crystallite size (nm)

β = total broadening = $[(\beta_{measured})^2-(\beta_{instrumentation})^2]^{1/2}$

λ = Wavelength (nm)

θ = Bragg angle (radian)

ε= micro-strain

The profile of XRD peaks was fitted by using the Pseudo-Voigt function for the computation of peak broadening. The total peak broadening was computed after subtracting the standard Silicon sample's broadening for neglecting the instrumental broadening.

3.4.5 Scanning Electron Microscopy (SEM): Morphology and Elemental Mapping

Scanning Electron Microscope is a powerful instrument and is normally used in the characterization of heterogeneous materials and surfaces. It characterized the morphology and microstructure of nanostructured powders and thin film materials too. It is generally used to characterize the topography, surface morphology, chemical composition, and particle size distribution. In SEM, the area to be examined is basically related to the surface and subsurface region of the specimen. The basic components of the SEM instrument consist of a vacuum chamber, electron gun, condenser lenses, objective lens, sample chamber, detectors, and sample stage. The half section of the SEM instrument is shown in Fig.3.4(a). The electron gun used is a source of electron beam having very high energy (few hundred eV to few keV). Electromagnetic condenser lenses are used to converge the electron beam (<5mm diameter). A high energy electron beam raster on the surface of the specimen with the help of scan coils to scan the specimen. Additionally, this high-energy electron beam also penetrates inside the specimen surface and undergoes electron volume interaction. These electron-volume interactions produced many useful signals including secondary electrons (SEs), back-scattered electrons (BSEs), Characteristics X-rays, Auger electrons, and photons of various energy. A schematic ray diagram of SEM along with the detectors for various signals is shown in Fig. 3.4(b). The BSEs are the result of elastic interactions and are reflected from the specimen surface with very high energy. Therefore, the BSE image can easily be distinguished in terms of the atomic numbers of the elements due to the contrast of the image. The SEs are ejected from ~10nm depth of the specimen surface. It gives

an inelastic interaction of the beam electron with the specimen. The BSEs have higher energy than SEs hence it is used for surface topography studies of nano-materials and thin films. Each signal is collected by their specific detectors so images are formed and displayed on the monitor. The three-dimensional appearance of these images is due to the large depth of focus of the SEM.

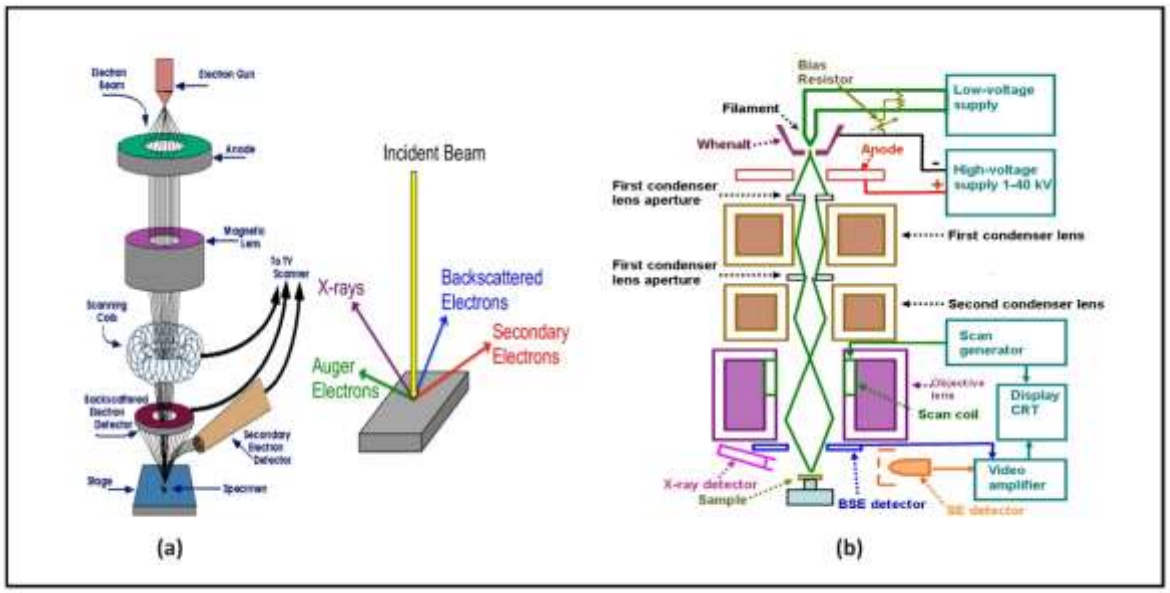

Fig. 3. 4 : (a) Schematic diagram of SEM, (b) Electron beam trajectory[154]

The present investigation examines microstructures and compositions of melt-spun ribbons, ball-milled powders, and sintered pellets by scanning electron microscope (Model: FEI Quanta 200F & NOVA Nano SEM 450) with an FEG source. The SEM instrument is equipped with an X-ray energy dispersive spectroscopy (EDS) detector for elemental analysis. The sample of ball-milled powder was prepared for SEM analysis by dispersing a few mg of powder in an ethanol and hexane solution and dropping it onto a clean Si wafer. Similarly, ribbons and sintered pellets are put on the sample stage with the help of a non-conducting carbon tap.

3.4.6 Transmission Electron Microscopy (TEM): Microstructure and Phase Analysis

Transmission electron microscopy is another very powerful and advanced characterization technique that gives highly magnified images of thin films and nano-structured materials by using parallel beams of electrons. TEM has achieved a unique distinction amongst micro-analytical techniques. The operating principles of TEM are similar to the visible light microscope, only a difference in electrons is used in TEM instead of light in the light microscope. The light microscope uses the wavelength of visible light therefore it is limited in terms of image resolution. The resolution of the visible light microscope is ~200 nm. In this context, TEM is superior to

the light microscope. The electrons that are used in TEM have much shorter wavelengths and give high resolution.

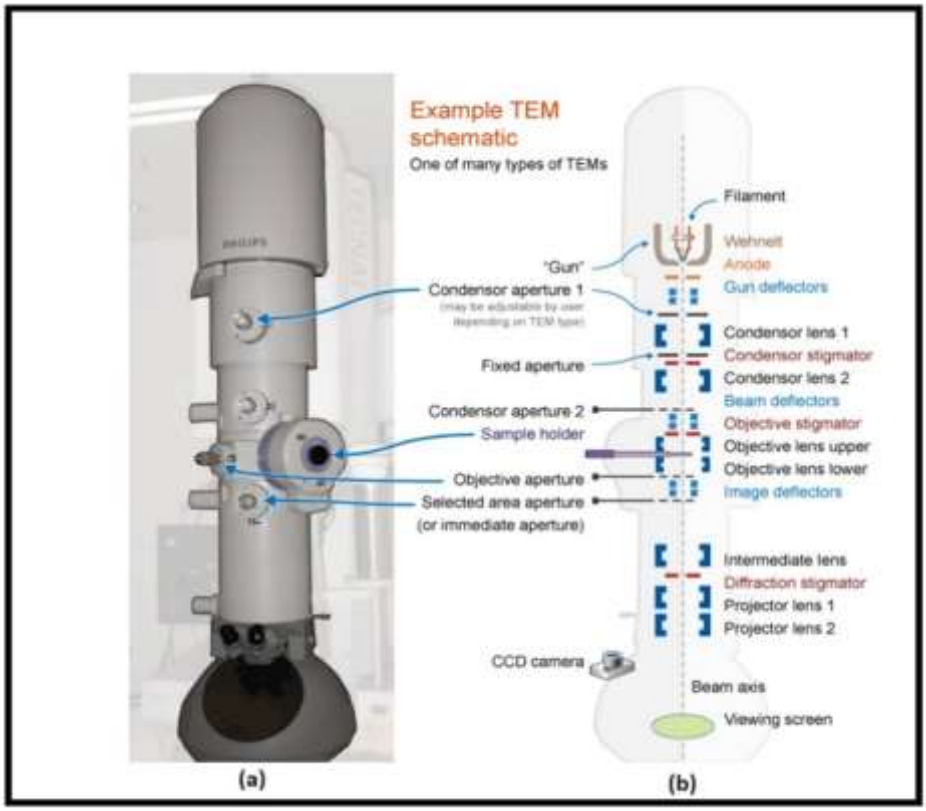

Fig. 3. 5: (a) Schematic picture of a TEM Overall cabinet assembly; (b) inside view of a TEM[155]

The electron beam with a high energy beam is accelerated with a voltage of ~200kV. The energy of the electrons can be controlled by calibrating the TEM to other voltage in the range of 80-300kV. One of the important advantages of the transmission electron microscope is its capability to explore the materials in reciprocal space as well as in real space (i.e., diffraction and imaging mode). The fundamental of the TEM imaging mode includes the quantum mechanical behavior of the interaction of the beam with the atomic potential of the materials. The electron beam getting transmitted through the specimen gets diffracted or scattered with the phase change. The transmitted wave becomes an object for the underlying projector lens. The projector lens amplifies the transmitted wave signal and projects it onto the fluorescent screen as a form of image. Fig. 3.5(a) shows the schematic representation of TEM and its inside view in Fig. 3.5(b). Fig.3.6, represents the path or trajectory of electron beam travel inside the TEM instrument in diffraction mode as well as imaging mode.

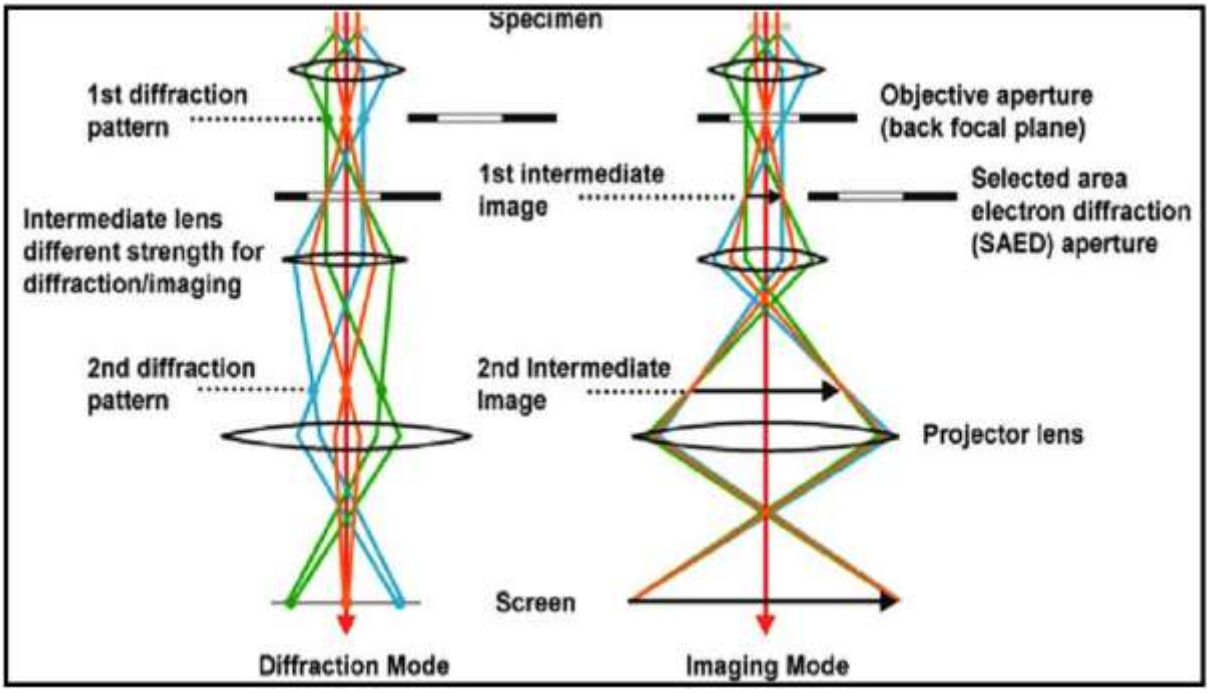

Fig. 3. 6: A schematic diagram of the trajectory of an electron beam in diffraction mode and imaging mode

In the present work, transmission electron microscopy (Tecnai G^2 T20) operating at 200kV was used for the investigation of amorphous and nano-crystalline phases of thin films of melt-spun ribbons. The TEM specimens of all four ribbon samples were prepared by grinding, dimpling and ion milling. The thinning of samples was done by precision ion milling using GATAN PIPS II. The samples were loaded at 6 degrees with 6keV operating voltage for 4 hours which was followed by 3 degrees with 3keV for half an hour and then 2 degrees with 2keV for again half an hour. The electron transparent region was first observed in the microscope attached to PIPS before loading into the TEM holder.

3.4.7 Differential Scanning Calorimetry (DSC): Thermal Characterization

The investigation of the crystallization of glassy alloys and also to know their thermal stability, it is very important to study the thermal behavior of such alloys. Differential scanning calorimetry (DSC,404 F3, Pegasus Netzch) was used for the identification of phase transformation temperatures (amorphous to crystallization), glass transition temperatures (T_g), crystallization temperature (T_x), melting temperature (T_m), kinetics, etc. In the present study, this instrument was used for the thermal characterizations of as-cast alloys, melt-spun ribbons, and 100h ball-milled powders. Approximately 50-60mg of as-cast alloys, 15-30mg of melt-spun ribbons, and 10-15mg

of powder samples were used for DSC measurements. The material under this investigation is typically subjected to a programmed temperature change and the effect due to thermal change in the materials is observed. The sample of DSC measurements was kept in an alumina Al_2O_3 crucible. The DSC calibration was first done with the help of In, Sn, and Al (99% pure). The DSC measurements and thermograph were obtained between room temperature to 1200 ºC. A constant heating rate of 20 ºC/min was used for finding the phase transformation and melting temperature. The thermal effects in the materials are observed in such a manner the temperature by which any event either absorbs or releases the heat under the continuous flow of purified nitrogen gas. This allows us to determine glass transition temperature, crystallization temperature, the study of order-disorder transitions, and chemical changes in the materials.

3.4.8 Indentation Characteristics: Mechanical property Measurements

The indentation technique is the most popular and commonly used for the testing of mechanical properties of materials. The purpose of micro-indentation hardness testing is to study the fine-scale (microscopic scale) changes in hardness. A very hard tip material (diamond) whose mechanical properties are known is pressed into a sample whose properties are unknown and to be determined. Micro-indentation hardness testing instrument is very useful for the materials engineer, it must be used with full skill and care. In the micro-indentation technique, a diamond indenter (Vickers indenter) of specific geometry is used to impress into the surface of the test specimen using a known load from 10g to 1000g.

In the present investigation, the study of hardness and elastic modulus of the as-cast alloys, melt-spun ribbons, SPSed pellets, and annealed ribbons are done by an instrumented micro-hardness tester (Anton Parr: MHT^3). A Vickers diamond indenter was used and at least ten indentations were taken for reproducing the results. Vickers indent has a 136º pyramidal diamond indent that forms a square indent. To determine micro-hardness and elastic modulus Oliver-Pharr method was used[156].We have applied the indentation load from 10mN to up to the fracture of the specimen with 20 sec of dwell time. The size of the indent is determined optically by measuring the two diagonals of the square indent. The main drawback of the Vickers test is it needs a mirror-like polished surface specimen so that the optical image has a clear image and makes to take an accurate measurement. For this samples were very fine or mirror-polished as per the procedure described in sub-section 3.4.2.